Journal of Constructional Steel Research 188 (2022) 107030

Contents lists available at ScienceDirect

Journal of Constructional Steel Research

journal homepage: www.elsevier.com/locate/jcsr

# Shake table testing of perforated steel plate shear wall having light gauge bolted infill panels

Daniel M. Dowden [a,*], Michel Bruneau [b]

[a] Dept. of Civil, Environmental and Geospatial Engineering, Michigan Technological University, Houghton, MI 49931, United States of America
[b] Dept. of Civil, Structural and Environmental Engineering, University at Buffalo, Buffalo, NY, 14260, United States of America

ARTICLE INFO

*Keywords:*
Bolted connection
Rocking connection
Self-centering
Steel plate shear wall
Perforated infill panels
Seismic performance

ABSTRACT

This paper presents the results of an exploratory study performed to examine the potential of using bolted connections between perforated infill panels and the boundary elements of steel plate shear walls. Perforated infill panels have the advantage over solid infills in that these panels can be detailed to minimize the forces imposed to the panel connections and surrounding boundary members. Furthermore, addition of perforations will accommodate the use of thicker perforated infill panels where solid infill thinner panels may not be practical. For such applications, bolted connections can be used to improve the replaceability of the web panels after a strong earthquake to facilitate rapid repairability. Hence, the combination of bolted connections with perforated infill panels could lead to an overall effective design solution for steel plate shear walls. This paper presents the results of a shake table test program on one-third scale three-story specimens as a proof of concept on the use of bolted perforated infill panels. The experimental results are compared to those obtained with conventional solid infill panels welded to the boundary elements. The results demonstrated that perforated SPSWs with slip-resistant bolted infill panels of thin cold-formed steel can provide a hysteretic behavior and seismic performance comparable to SPSWs having with conventional solid infill panels with welded connections.

## 1. Introduction

Steel plate shear walls are effective in resisting lateral loads due to wind and earthquakes acting on building structures. For low- and medium-rise building applications or structures, the thickness of the wall infill panels required to develop the required story shear strength is small, often much smaller than the minimum hot rolled plate thickness (typically 5 or 6 mm/0.197 or 0.236 in.) required for handling and welding in the shop or at the site. When selecting such overstrength plates for seismic resistance, beams, columns, connections, and foundations must then be designed for larger forces to ensure that plate yielding can be achieved as intended in codes, which negatively affects the cost-effectiveness of the system. Furthermore, using minimum plate thickness over part of or the entire height of a multi-story structure is likely to result in uneven distribution of the inelastic demand in the frame, which is undesirable in terms of seismic performance.

Berman and Bruneau [1] demonstrated that stable and ductile steel plate shear wall response can be obtained with flat light gauge steel infill panels, provided that ductile light gauge steel is used. The test specimen was built with an infill panel approximately 1.0 mm thick that was fully welded to WT sections bolted to the perimeter beam and column members. The use of such thin plates represents an effective way of alleviating the problems and cost increases caused by wall overstrength in a structure. However, because light gauge steel sheets are only available in discrete thickness increments, typical multi-story designs are expected to exhibit sharp variations in lateral resistance at levels where the plate thickness is varied, as well as uneven demand-to-capacity ratios along the building height. This shortcoming can be overcome by using infill panels designed with circular perforations [2]. The perforations are regularly spaced to form diagonal strips acting in tension. Purba and Bruneau [3] proposed details and design recommendations for the seismic design of such perforated walls. These have been implemented in seismic design provisions in both the U.S. and Canada. Recommended details are summarized in Fig. 1. In the AISC-341 seismic provisions [4], based on imperial units, the factored resistance of perforated infill panels, $V_r$, (or $V_n$) is given by:

$$V_r = 0.42\left(1 - 0.7D/S_{diag}\right)w\phi F_y L_i \tag{1}$$

where $D$ (in.) and $S_{diag}$ (in.) are the diameter and spacing of the

* Corresponding author.
*E-mail addresses:* dmdowden@mtu.edu (D.M. Dowden), bruneau@buffalo.edu (M. Bruneau).

https://doi.org/10.1016/j.jcsr.2021.107030
Received 13 May 2021; Received in revised form 27 October 2021; Accepted 28 October 2021

perforations, $w$ (in.) is the plate thickness, ϕ is the resistance factor (= 0.9), $F_y$ (ksi) is the specified minimum steel yield strength and $L_i$ (in.) is the net panel length between columns. The equation assumes an inclination angle of 45° for the tension field, as illustrated in Fig. 1. At every level of a structure, the thickness of the light gauge infill panel and the size and arrangement of the perforations can be selected such that the shear strength of the infill panels closely matches the required story shear demand, thus minimizing unnecessary wall overstrength and achieving uniform strength-to-demand ratio in the structure.

To minimize handling and ensure adequate welding of the thin plates in actual building applications, steel plate shear wall units can be pre-assembled in the plant prior to shipping to the site. Such a pre-fabricated wall design is illustrated in Fig. 2. This office building was built in Montreal, Quebec, a region of moderate seismicity typical of eastern North America. For this 4-story structure, each shear wall was fabricated in one piece and shipped to the site. The walls were fabricated using only two different plate thicknesses and the shear strength at every floor of every wall was adjusted by modifying the perforation pattern. Variable web perforation designs can now be easily accomplished using plasma cutting equipment.

Although effective, it is believed that this wall design could be improved further by using bolted connections on the perimeter of the infill panels. To leverage the advantages of a bolted versus welded infill web panel connection to the boundary frame, SPSWs with bolted infill web panels could be prefabricated in the shop. This would eliminate bolt fit-up issues in the field while also substantially reducing the construction schedule by leveraging on the rapid constructability of using pre-fabricated wall panels. Also a significant benefit, it would eliminate concerns related to the welding of thin light-gauge steel in a manner that can develop the full yielding capacity of the infill web panel. Panels damaged during construction or after a strong seismic event could be easily replaced at the site. For the latter, this would greatly simplify the process and eliminate the high costs resulting from flame cutting and welding existing and replacement infill panels, respectively, in an existing building. Bolt holes on the infill perimeter can be plasma cut at the same time as creating the web perforations. One perceived drawback is that, in seismic design, the connections must develop the expected yield tensile strength of the infill panels, which could be more difficult to achieve with bolted connections. However, at the same time, it may be easier to design bolted infill connections in perforated SPSWs as a consequence of the reduction in force demand on those connections due to the perforations. Past experiments have shown that infill panel yielding can be achieved with bolted connections (e.g., [5,6]), whereas in the latter a bolted clamping bar was used to connect light gauge infills), and a few SPSWs with bolted infills have been implemented in practice [7].

This paper presents the results from a shaking table test program conducted to experimentally validate the feasibility of using bolted connections for perforated light gauge steel sheets used as thin infill panels for steel plate shear walls designed for ductile seismic response. The bolted perforated infill panel was limited to a single test specimen. The purpose of this test was to provide a proof of concept of a bolted perforated infill panel and compare the system response to a companion welded connection solid infill panel. A broader testing program investigating system behavior with different bolted connection and infill perforation configurations was beyond the scope of work. The test was

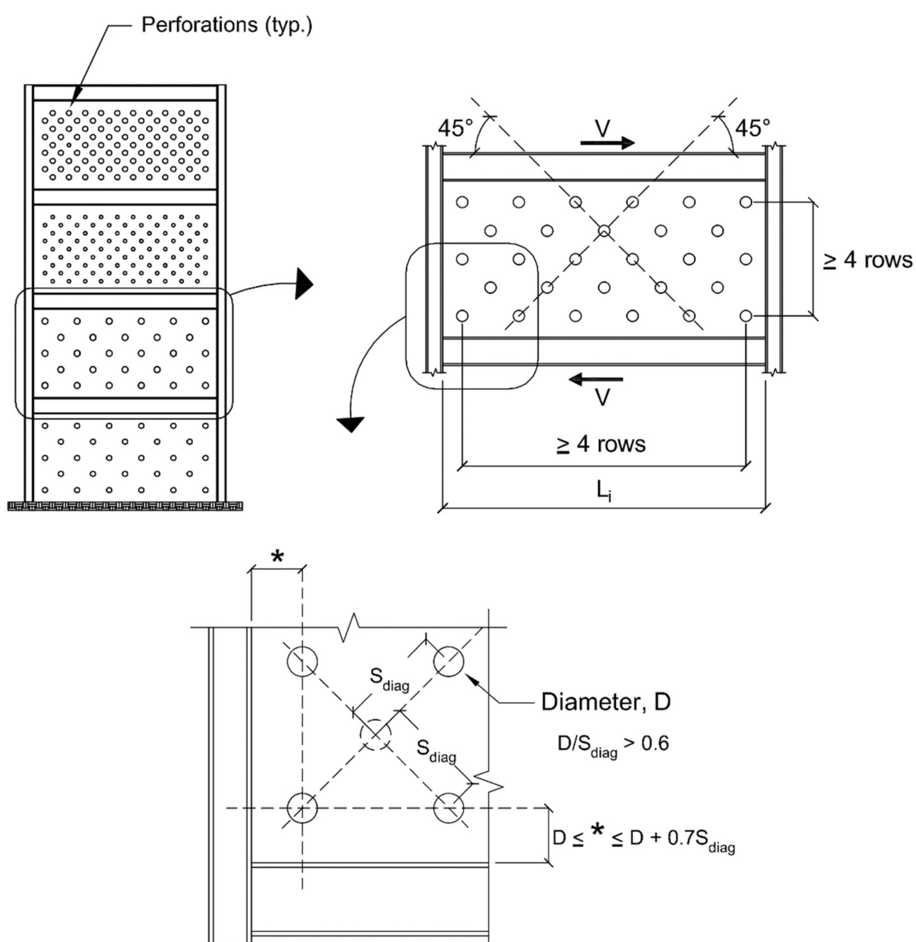


**Fig. 1.** Perforated steel plate shear wall: overall view and detailing requirements.

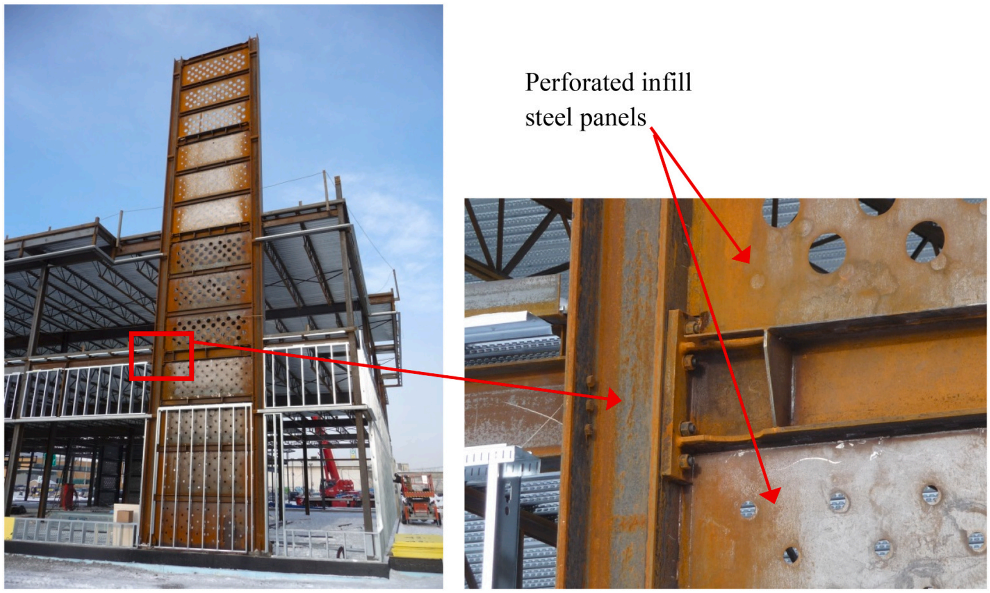


**Fig. 2.** Four-story perforated steel plate shear wall with RBS-End plate beam-to-column connections (Courtesy of Eric Lachapelle, LAINCO Inc.).

carried out on a one-third-scale 3-story steel plate shear wall specimen, as part of a wider test program that included solid and welded infill panels, allowing direct comparison.

## 2. Bolted connections for infill panels

### 2.1. Design assumptions and seismic induced force demand

A simple single-shear bolt with a nut and washer is examined in this study and schematically presented in Fig. 3. In that figure, at level 1, the infill panel is bolted to a fish plate that is welded to the perimeter beams and columns of the SPSW. Note that the fish plate pre-welded to the beams and columns is already a standard detail commonly used to facilitate fabrication of steel plate shear walls in the field [7], and that the difference here is that the infill plate is bolted to it, instead of welded. Standard holes are used and the bolts are installed such that the nut and washer are placed on the infill panel side. The bolts are regularly spaced on the perimeter of the panel. Under lateral loads, buckling of the infill panel is anticipated and story shear resistance of the infill panel is assumed to be provided essentially by tension field action. When perforations are used, AISC 341 requires that the perforations be arranged along a grid pattern inclined at 45°, which defines the assumed inclination of the tension forces in the panel.

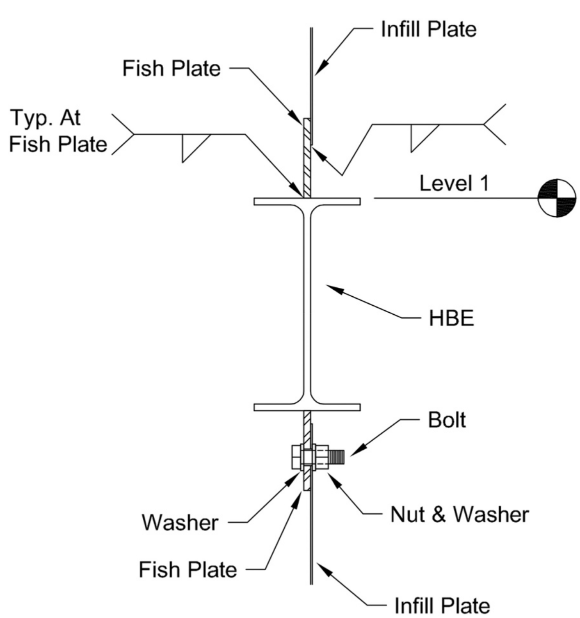


**Fig. 3.** Infill panel connection to HBE beam.

It is assumed that the bolts and perforations are arranged such that an average uniform tension is applied to the bolted connection. This is a simplifying assumption reasonable for design purposes; although this could be further investigated through component testing, this was beyond the current scope of work. In that case, as illustrated in Fig. 4, the tensile force $T_f$ per bolt is determined from the average tensile stress acting on a strip of width $0.71a$, where $a$ is the bolt spacing. In seismic design, the connection of the infill panel to the boundary elements must resist the effective expected tensile strength of the plate. This capacity is determined from the probable, or expected steel yield strength, $R_yF_y$, and accounts for the presence of the perforations. From [4], modified for the bolt layout considered here, the design tension force for each bolt can be determined from:

$$T_f = \left(1 - 0.7D/S_{diag}\right) wR_yF_y(0.71a) \tag{2}$$

where $R_y$ = ratio of expected yield stress to the specified minimum tensile strength, $F_y/F_u$; and $a$ = on center spacing of bolts.

All failure limit states must provide adequate strength to resist this force. In bearing connections, this includes shear strength of the bolts, net section tension strength, as well as bearing and end tear-out strength of the infill panel. Failure may also occur in the fish plate and its welded connection; however, these failure modes are well documented and not discussed herein. For this project, the 2012 Edition of the North American, jointly developed AISI-100/CSA 132 specification for the design of cold-formed steel structural members [8] was used to determine the ultimate strength of thin cold-formed steel sheets of the type considered here (i.e., thinner than 4.8 mm/0.189 in.). Bolt strengths were calculated per the AISC 360 specification [9] assuming threads were included in the bolt failure shear plane. Two of the potential failure modes involving the infill panel are illustrated in Fig. 4 to highlight some assumptions adopted in this case.

As shown in Fig. 4, net section area was calculated considering that the single row of holes along the connection performed as staggered holes from the perspective of the diagonal tension strip. In this case, the shear lag factor (per AISI-1002012, Table E6.2-1) used to calculate the

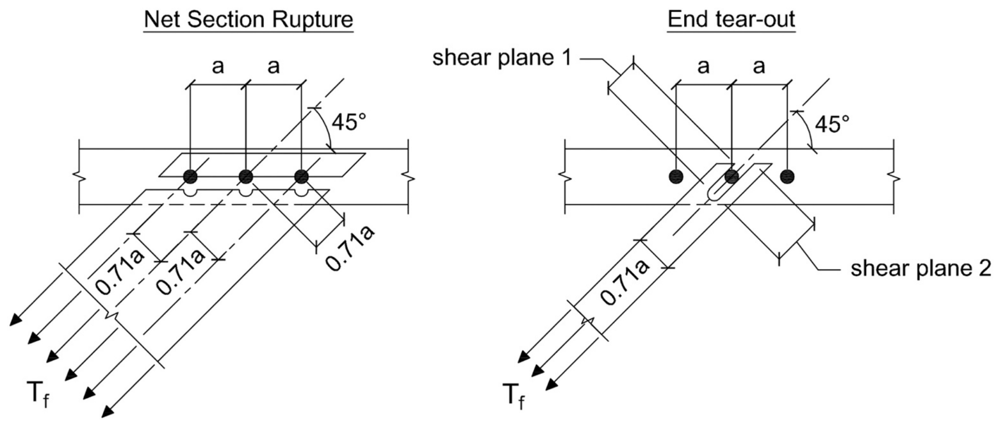


**Fig. 4.** Connection failure modes involving the infill panel.

effective net tension area could have been taken as 1.0, as applicable to flat sheets connections having staggered hole patterns. However, for the design considered here, the more conservative value of this factor is applicable to single rows of connectors perpendicular to the force (with washers provided under the bolt head and the nut). For the end tear-out limit state, the net length of the shear failure planes was conservatively taken as the shorter of the two shear planes (i.e., shear plane 1), as shown in Fig. 4. Furthermore, for the plate bearing resistance, the AISI-100 value (calculated per Article E3.3.1) was reduced by 20% as suggested by AISC 341-10 to account for the more severe bearing demand expected under cyclic seismic excitations.

Finally, as commonly done in seismic design, since the force demand and the resistance are both determined from the same material for all three failure modes, as permitted in the AISC 341-10 seismic provisions, the expected tensile strength, $R_tF_u$ (where $R_t$ = ratio of the expected tensile strength to the specified minimum tensile strength $F_u$), was therefore used to assess the connection strength instead of the corresponding minimum specified value. For the same reason, the approach adopted for the design of pre-qualified moment frame beam-to-column connections [10] is also applied to establish the resistance factor applicable to each limit state: $\phi_d = 1.0$ for a ductile failure mode, such as bolt bearing, and $\phi_n = 0.9$ for non-ductile failure modes such as net section rupture and end tear-out.

A systematic procedure could easily be developed using the above limit states to identify the "design space" of admissible solution, or to develop design aids, but that is beyond the scope of this paper. Note that all bolts were also pre-tensioned, achieving a slip-resistant connection. If bolt slip is prevented, it is expected that tension in the infill panel will be mostly transferred to the fish plate by friction between the two plates, rather than by bearing of the infill panel against the bolt, shear in the bolt, and bearing of the bolt against the fish plate. Furthermore, for thin plates, resistance against slippage can be the result of friction along two planes, one between the infill and fish plates and one between the infill panel and the bolt washer, where the tension transferred along the second slip plane would then be transferred to the fish plate through bolt shear (Personal Communication, Professor Robert Tremblay, Ecole Polytechnique, Montreal 2016). This would result in additional slip resistance compared to the value assuming only one slip plane, although this additional strength was not necessary in this case. Here, strength of a slip-resistant single-shear connection with pre-tensioned high-strength bolts was calculated as provided by AISC-360 for Class A, clean mill scale, faying surface conditions.

## 3. Shake table test program and experimental results

Shake table testing of the proposed bolted perforated SPSW was performed using specimens adapted from a previously completed test program investigating a proposed self-centering steel plate shear wall (SC-SPSW) system [11–13]. Self-centering SPSWs differ from conventional SPSWs in that the rigid beam-to-column connections are replaced with post-tensioned (PT) rocking beam-to-column connections. The PT rocking connections provide frame self-centering and also allow decoupling of the hysteretic energy dissipation components to easily replaceable elements. Similar self-centering systems were previously proposed on steel moment frames [14–17]. The SC-SPSW specimens of the previously completed test program consisted of 1/3 scaled, 1-bay, 3-story frames, detailed with three different PT beam-to-column rocking joint connections [18]. The prototype building used for this project to design the test specimens, was modeled after the 3-story prototype building used in the SAC Steel Project [19] for a project site located in Los Angeles, CA. For the test specimens, the earthquake spectral response acceleration parameters were based on the 2009 NEHRP seismic hazard maps. Further information on the test specimen design is provided in [12]. For the current purpose, the columns or vertical boundary elements (VBEs), beams or horizontal boundary elements (HBEs), and post-tensioning details from this original test program were re-used and modified to build a perforated SPSW with bolted infill panels. This specimen was then subjected to a shake table test series to validate the seismic behavior of the perforated thin infill web panels with slip-critical bolted connections to the boundary frame.

### 3.1. Test program and specimen details

The results presented here are for two test specimens referred to as frame NZP and NZW, respectively. This SC-SPSW system is detailed with the NewZ-BREAKSS PT beam-to-column rocking connection [20]. A detailed description on the self-centering behavior and frame kinematics of frame NZP and NZW with this joint connection is provided in [21]. This connection, which results in rocking about the top beam flanges only, was inspired by connections proposed previously by others [22–25] to eliminate the PT boundary frame expansion (i.e., increase in distance between frame column centerlines) that occurs with other investigated rocking connections referenced earlier.

A series of three shake table tests investigating different infill web panel configurations had already been performed using the boundary frame of frame NZP [13]. After each test, the damaged infill panels were replaced for the next test series, which also served to validate the reusability of the PT boundary frame and the use of replaceable hysteretic energy dissipating elements. For frame NZP here, two welded solid web panels were used in stories 2 and 3, as was done in previous tests. However, the infill panel in the first story had perforations and bolted connections to the boundary frame. Providing a perforated bolted infill plate at the ground level only, provided an opportunity to provide a more direct comparison of an individual perforated infill plate to a solid one in otherwise similar walls. The perforated infill web panel was designed to have a strength approximately equivalent to that of the solid

22-gauge infill web panel used in the previous tests at story level 1. Thus, the target goal was to have frame NZP to be approximately equivalent to the previously tested specimen, frame NZW, which had solid infill web panels welded to the boundary frame over all stories. A comparison of frames NZW and NZP is presented in Fig. 5, and details of the first-story panel for specimen NZP are given in Fig. 6. Note that for use in frames with beam-to-column rocking connections, it is important that the location of the perforated holes be aligned with the corner cut-outs as shown in Fig. 6, since the radial corners are themselves a natural perforation in the panel in the form of a quarter-circle.

The test specimens consisted of (U.S. designation) W8x18, W8x15, and W8x18 for Level 3, 2, and 1 beams, respectively, W6x25 for the columns, ASTM A992 [26] material for all boundary frame members, and 12.7 mm (0.5 in.) diameter ASTM A416 [27] grade monostrands for the PT. A total of two monostrands were provided at each beam end (one located on each side of the beam web) located at distance of 64 mm below the mid-depth of the HBE. An initial target PT force of approximately 40 to 45% of the PT yield strength for each monostrand was provided. Solid infill panels were ASTM A1008 cold-rolled steel [28]. The perforated panel was made from a solid infill panel using a plasma cutting machine. Further information on the test specimen design and evaluation of relevant material properties is provided in [12,18].

The test setup used an existing modular lateral bracing system developed at the University at Buffalo site for the experimental testing of scaled specimens [29] and is referred to as the Gravity Mass Frame (GMF). The GMF system is designed to be a self-contained structure that can support its own gravity weight, has lateral stiffness and stability in its primary transverse direction, but has essentially no lateral stiffness in its longitudinal direction (facilitated by semi-spherical rocker plates at the top and bottom of the GMF columns, of which a photograph is presented in Fig. 7). Each set of gravity columns supports a 89 mm (3.5 in.) thick steel plate weighing approximately 38 kN (8.5 kips) each, providing an approximate seismic weight of 76 kN (17 kips) per level, for a total of 227 kN (51 kips). Inertia forces are transferred from the GMF mass plates to the specimen at the diaphragm connections at the ends and at mid-span of each HBE, as shown in Fig. 7. The test setup on the shake table and specimen prior to testing is shown in Fig. 8. Further

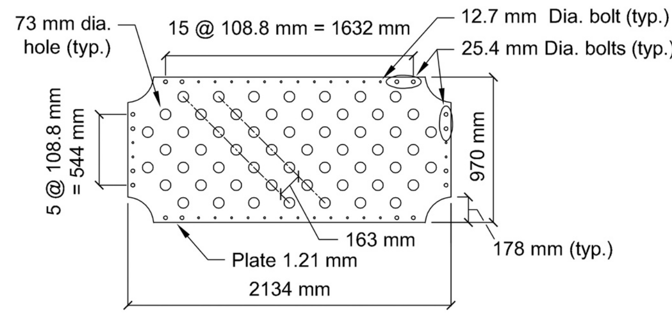


**Fig. 6.** Detail of the first-story perforated infill panel of the NZP specimen.

information on the test setup, scaling procedures, and instrumentation used is provided in [12].

The first-story perforated panel was designed to develop the same shear yield strength $V_y$ as the panel used in frame NZW. The fully yielded shear strength, $V_y$, of an infill panel can be obtained from Eq. (1) by using a factor 0.5 instead of 0.4 and setting $\phi = 1.0$. For the original specimen, 0.76 mm thick (22 GA) steel sheet with measured $F_y = 195$ MPa (28 ksi) and $D/S_{diag} = 0$ were used, which gives $V_y = 129$ kN (29 kips) with $L_i = 1740$ mm (68.5 in.). For the NZP specimen, 1.21 mm thick (18 GA) steel with measured $F_y = 183$ MPa (27 ksi) was used and the perforations were detailed to obtain $D/S_{diag} = 73/163 = 0.45$, which led to $V_y = 132$ kN (30 kips).

ASTM A325 [30] bolts spaced 108.8 mm (4.283 in.) apart were used on the perimeter of the frame NZP infill panel. The resulting expected force $T_f$ per bolt upon panel yielding is 11.7 kN (2.6 kips). The bolts were 12.7 mm (0.5 in.) in diameter, except for the last two bolts at the corners which had a diameter of 25.4 mm (1 in.). For the 12.7 mm (0.5 in.) bolts, the calculated factored shear resistance and slip resistance are 35.1 and 15.0 kN respectively, hence larger than $T_f$. Using the measured $F_u = 312$ MPa (45 ksi) for the infill panel, the factored effective net tension strength, bearing strength, and tear-out strength calculated as indicated earlier were respectively equal to 15.4 (3.46), 11.3 (2.54), and 12.4 kN (2.79 kips). Hence, bearing and end tear-out failure modes were critical

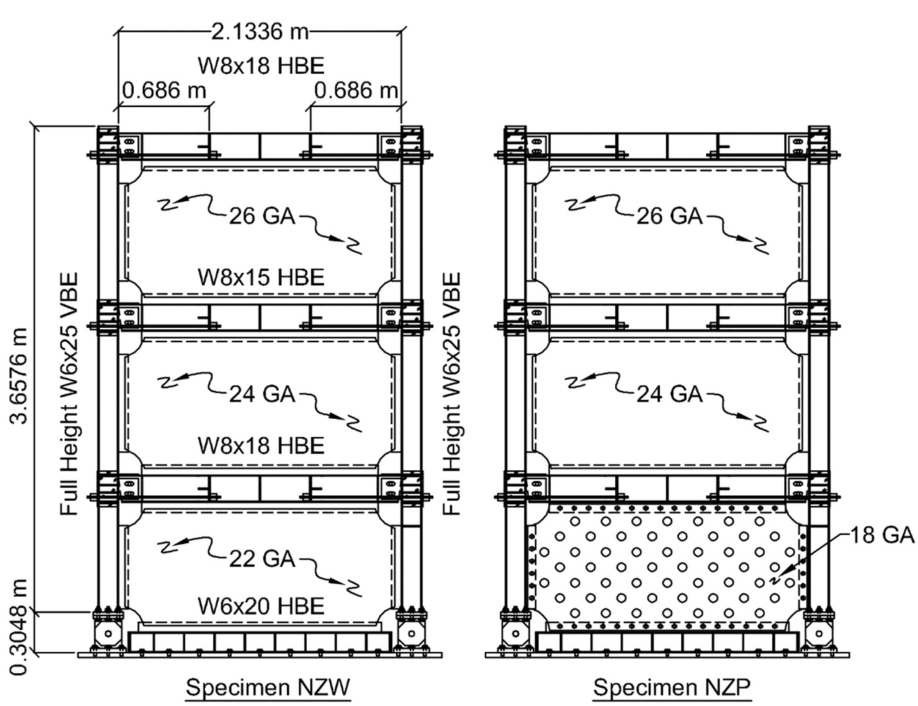


**Fig. 5.** Three-story steel plate shear wall test specimens: solid and welded infill panels at every level (NZW) and specimen with perforated and bolted web panel at the first level (NZP).

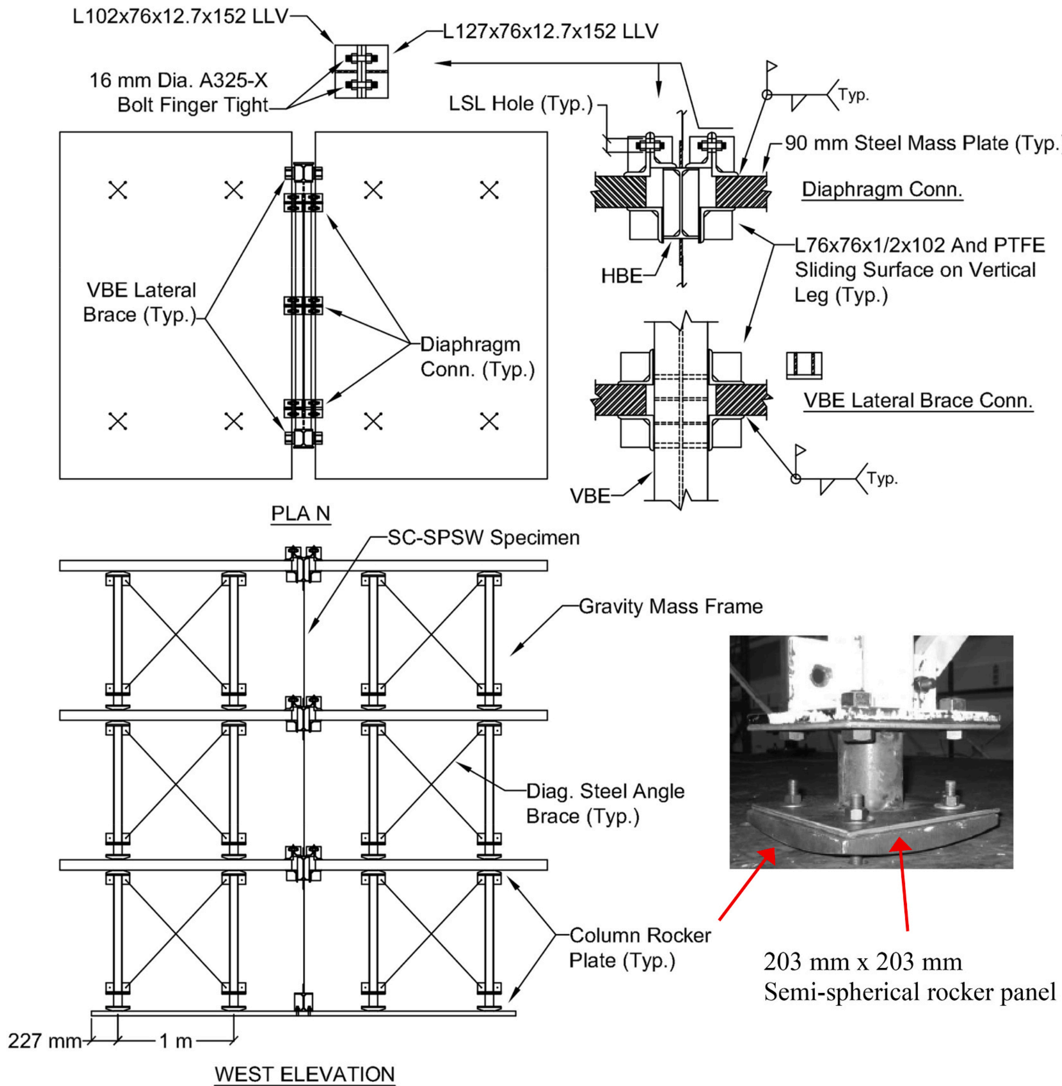


**Fig. 7.** Test setup details.

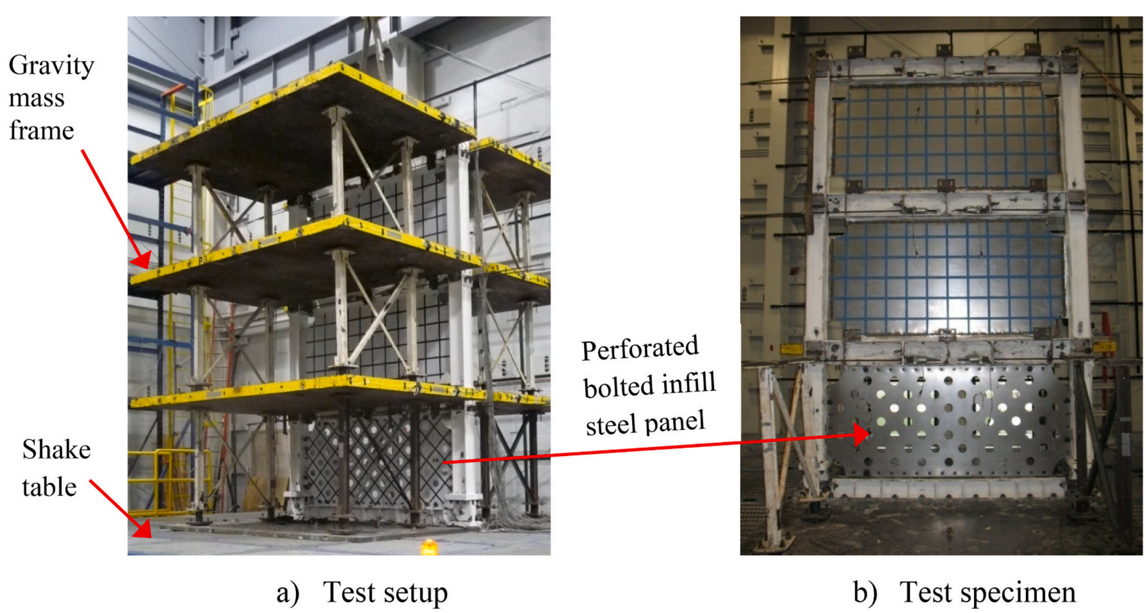


**Fig. 8.** Frame NZP prior to testing.

for the specimen. However, the two strengths were close to or slightly larger than $T_f$ and adequate performance was expected. Moreover, because factored bolt slip resistance (15.0 kN or 3.37 kips) was higher than $T_f$, it was expected that no slip would occur, and the connection would be protected against the risk of bearing and tear-out plate failure.

As was shown in Fig. 6, radial cut-outs were provided at the four corners of the infill panels to delay infill panel tearing initiating from the corners due to large tensile web plate strains and out-of-plane buckling along the plastically elongated free-edge of the infill panel corner cut-outs [31], which are further exacerbated by the formation of a gap at the beam-to-column joints. Larger bolt sizes were used in the corner to resist the tension loads generated in strips coinciding with the cut-outs. A proposed analytical equation to facilitate joint detailing to delay such infill panel tearing effects and sizing of the corner reinforcement bolts, can be found in [21].

### 3.2. Loading protocol

A spectra-compatible synthetic ground motion (GM) was generated for use in the shake table tests [13] and presented in Fig. 9 along with a comparison of the corresponding GM spectral accelerations with the target design response spectrum (DRS). The loading sequence for frame NZW and NZP is summarized in Table 1 for frames NZW and NZP. As shown in that table, the loading protocol consisted of amplitude scaling the synthetic GM, beginning with low level amplitude intensities, and for subsequent ground motions with increased scaled amplitudes. Testing continued by scaling the GM up to the safe operating limits of the shake table, determined by monitoring the overturning moment and base shear demands of the test specimen. Furthermore, as indicated in the table, for frame NZW, the tests concluded with the GM scaled to 50% of DRS (arbitrarily assuming aftershocks of these intensities) to investigate frame response after the infill web panels have yielded significantly. For frame NZP, additional aftershock levels of 100% and 120% GM were also conducted. To establish natural frequencies of the specimens and quantify changes in dynamic properties, white noise (i.e., an acceleration-controlled flat-spectrum broadband random motion) identification tests were conducted prior to each GM amplitude and at the conclusion of each test. Note that for the experimental results presented subsequently, a positive drift corresponds to an eastward drift direction.

### 3.3. Experimental results and discussion

The base shear normalized by the total effective seismic weight (i.e., $W = 227$ kN or 51 kips) versus roof drift resulting from the concatenation of all GM amplitudes and the residual drifts for all individual GM amplitudes are shown in Fig. 10. Given the typical code-specified 0.2% out-of-plumb construction tolerance, a maximum value of 0.2% residual roof drift was used as the criterion for frame recentering. From Fig. 10, it is observed that recentering was achieved for all GM amplitudes. It is noted that although re-centering was achieved, this does represent a potential $+/-$ 0.2% change in interstory drift from the original installed

**Table 1**
Loading protocol.

| Frame NZW | | | Frame NZP | | |
|---|---|---|---|---|---|
| GM Amplitude[a] | PGA | | GM Amplitude[a] | PGA | |
| | %GM | g | | %GM | g |
| WN | – | 0.10 | WN | – | 0.10 |
| 1 | 10 | 0.07 | 1 | 15 | 0.11 |
| WN | – | 0.10 | WN | – | 0.10 |
| 2 | 25 | 0.18 | 2 | 25 | 0.18 |
| WN | – | 0.10 | WN | – | 0.10 |
| 3 | 50 | 0.36 | 3 | 50 | 0.36 |
| WN | – | 0.10 | WN | – | 0.10 |
| 4 | 75 | 0.53 | 4 | 75 | 0.53 |
| WN | – | 0.10 | WN | – | 0.10 |
| 5 | 100 | 0.71 | 5 | 100 | 0.71 |
| WN | – | 0.10 | WN | – | 0.10 |
| 6 | 120 | 0.85 | 6 | 120 | 0.85 |
| WN | – | 0.10 | WN | – | 0.10 |
| 7 | 140 | 1.00 | 7 | 140 | 1.00 |
| WN | – | 0.10 | WN | – | 0.05 |
| 8 | 140 | 1.00 | 8 | 140 | 1.00 |
| WN | – | 0.10 | WN | – | 0.10 |
| WN | – | 0.10 | 9 | 50 | 0.36 |
| 9 | 50 | 0.36 | WN | – | 0.10 |
| WN | – | 0.10 | 10 | 100 | 0.71 |
| | | | 11 | 120 | 0.85 |
| | | | WN | – | 0.1 |

[a] WN - white noise excitation.

infill web panel condition. To accommodate replacement post-event, the bolt holes in the HBE fish panels could be detailed with oversized holes to accommodate infill web panel replacement. Another approach could be to field install the holes in the replacement infill web panels. A comparison of the incremental dynamic response of frames NZP and NZW is shown in Fig. 11. As presented earlier, the two frames are approximately equivalent, and the response should be similar. It is observed that the peak base shear demand and roof drifts are almost identical up to the 120% GM. Thereafter, it is observed that roof drifts are noticeably larger for frame NZP (i.e., at the first 140% GM), but the corresponding peak base shear demand remains approximately the same between the two frames.

The difference in response after the 100% GM is attributed to the perforated holes provided at the Level 1 infill web panel for frame NZP. In particular, some compression strength is developed by the infill panels due to the random folding of the panel. More specifically, when the infill panel yields, it develops a sort of "corrugated" shape upon reaching plastic deformations that exceed the previous deformations reached, which can then provide some stiffness in compression (equivalent to a temporary compression-strut). This strut effect of the infill web panel upon significant yield is significantly less in the perforated infill panel compared to the solid infill web panel; indicated by larger drifts observed in frame NZP. For example, the maximum roof drift was approximately 2.7% at the 140% repeat GM amplitude, where at the

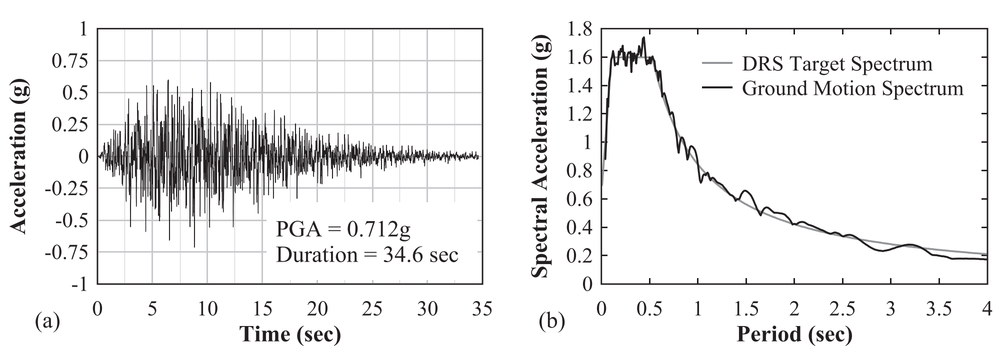


**Fig. 9.** (a) Generated synthetic ground motion; (b) ground motion spectral acceleration.

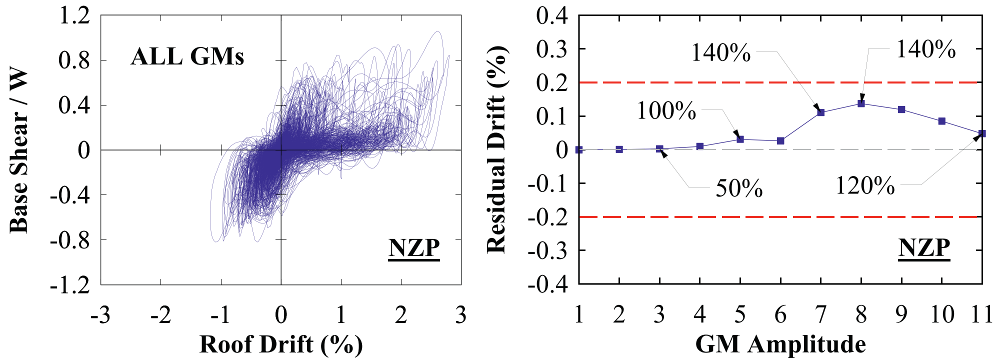


**Fig. 10.** Frame NZP – global response.

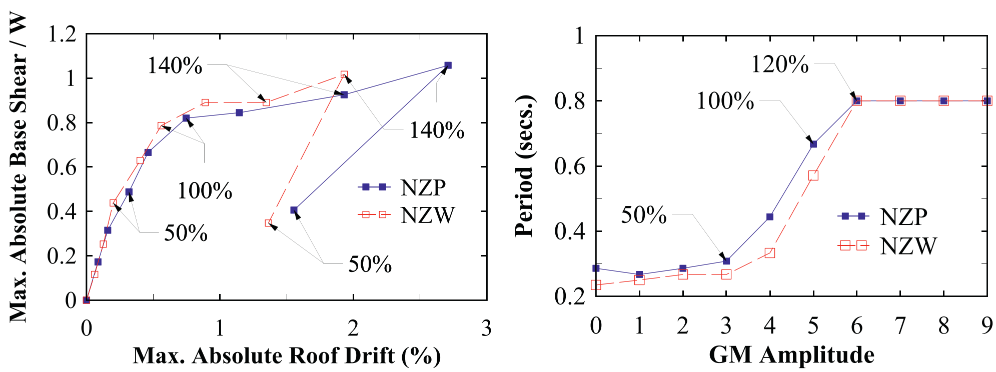


**Fig. 11.** Frame NZP versus NZW – incremental dynamic response.

corresponding GM amplitude for frame NZW it was 1.9%. However, the observed noticeable disparity in roof drift due to reduced compression strut effect for the perforated infill panel was more apparent at the 140% repeat ground motion (i.e., repeat of the approximate maximum considered level earthquake intensity), which would be a highly unlikely loading scenario in an actual building. For the design level earthquake (100% GM) the difference in roof drifts between frame NZW and NZP were significantly less and the drifts were comparable as

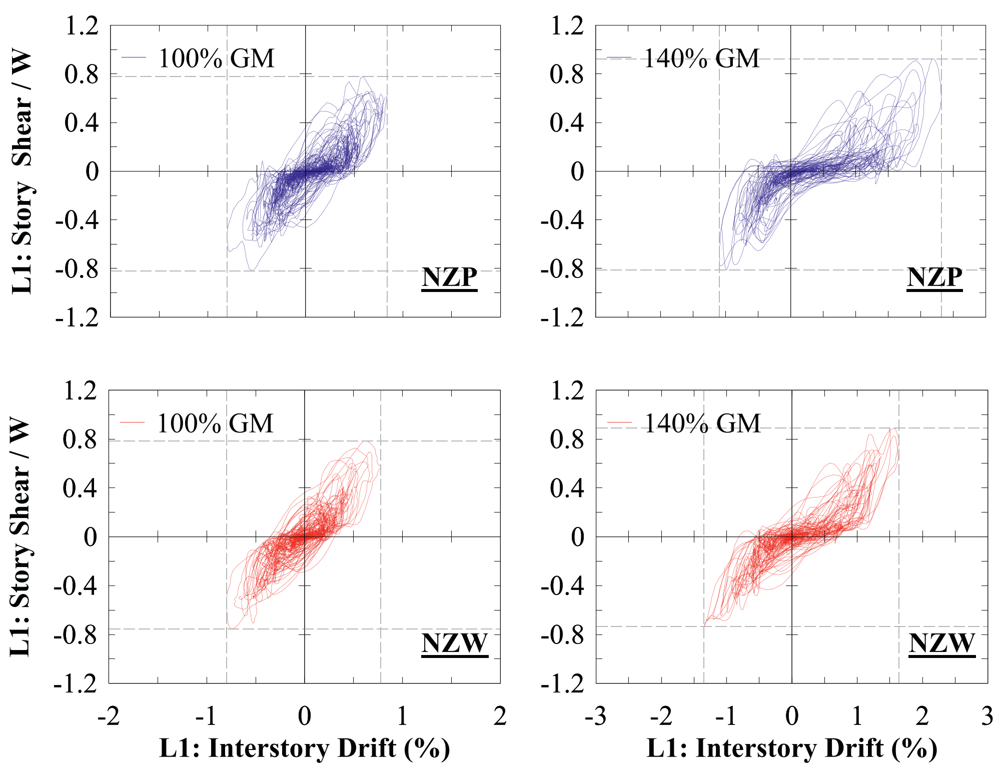


**Fig. 12.** Frame NZP versus NZW – Global Response – Select GMs.

observed in Fig. 11. Accordingly, the results suggest that the observed reduced compression strut effect in frame NZP compared to frame NZW for a design level earthquake, does not have a significant effect on frame drift response.

Furthermore, the individual story shear versus interstory drift at Level 1 is shown in Fig. 12 for the 100% and 140% GM, which provides a more direct comparison of response history between the two frames. Note that in the figure, for convenience, dashed reference lines are provided that locate the peak base shear and roof drift responses. It is observed that the overall general response history is comparable with the difference of increased roof drift noted for the 140% GM. No bolt slip or tearing of the infill web panel occurred at the bolted connections on the boundary frame, whereas some minor panel tearing was observed at Levels 2 and 3 infill web panels. Pre- and Post-test photographs of the perforated infill panel deformations, condition at the corner bolt holes, and interior located bolt holes is shown in Figs. 13–15, respectively.

In Fig. 13a and b, the inelastic damage of the bolted infill web panel can be visually identified by comparison of the black painted diagonal stripes. Note that the white-washing on the infill web panel was intended to provide a contrast with the diagonal painted stripes between the infill perforations and not to measure the level of inelastic damage (which will be addressed later). Figs. 14 and 15 show from a visual inspection that no apparent bolt slip or connection damage occurred during the tests, providing some support to the design equations used for the bolted infill web panel connections used in frame NZP.

In this test program, the setup was not designed to push the specimen to collapse (in order to stay within the safe operating limits of the shake table) and no information could be obtained on the ultimate failure mechanism. However, the shake table tests presented provided a valuable proof-of-concept of the proposed system. More specifically, the slip-critical bolted infill web panel connections performed as desired. Bolt slip and connection failure was prevented while substantial inelastic behavior developed in the bolted infill web panel. In particular, frame NZP was severely tested, being subjected to a total of eleven individual earthquake loadings, six of which were earthquakes of equal or greater severity than the one corresponding to the design ground motion. In between each of these ground excitations, the bolted infill web panel connections were never retightened. Evidence of achieving inelastic behavior in the infill web panels is observed in Fig. 11 where the fundamental natural period of the frame progressively shifted from 0.23 s to 0.8 s (as expected in this type of SPSW). Furthermore, to measure the approximate axial strains of the bolted infill web panel (as a measure of the inelastic response), string potentiometers were installed along a diagonal parallel to the perforated holes where 1.8% and 2.3% axial strains were measured at the 12.7 mm and 25.4 mm diameter bolt locations. The excellent performance exhibited throughout this series of tests up to 140% GM and the excellent correlation with the performance of a similar specimen with a solid infill web panel, provide evidence that thin infill panels with bolted perimeter connections can represent an alternative solution for seismic steel plate shear wall designs.

## 4. Conclusions

Perforated SPSWs having light gauge steel panels have been built as an effective structural system to resist earthquake forces (e.g., for low-rise buildings or buildings in regions of moderate seismicity). Some steel fabricators have suggested that further efficiencies in the assembly (and thus cost-effectiveness) can be achieved by using bolted connections on the perimeter of the infill panels instead of welds. On that basis, a shake-table test program was conducted using a previously tested third-scale, self-centering steel plate shear walls in which the solid infill panel at the lower story was replaced by the proposed bolted, perforated web panel. The satisfactory performance of the system was confirmed though testing under repeated ground accelerations, progressively scaled up to 140% of design level, and subsequent “aftershocks” of varying severity. The experimental results demonstrated that perforated SPSWs with slip-resistant bolted infill panels of thin cold-formed steel can provide a hysteretic behavior and seismic performance comparable to SPSWs having solid, welded infill panels. Further experimental and numerical studies are required to fully characterize the ultimate strength and behavior of these slip-critical connections. More specifically, additional small-scale tension tests to failure would allow to fully validate

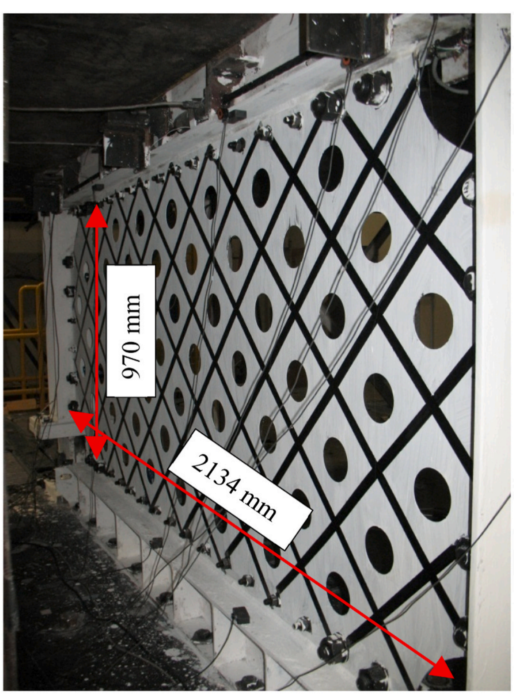


a) Pre-test

b) Post-test

**Fig. 13.** First-story infill panel of the NZP specimen.

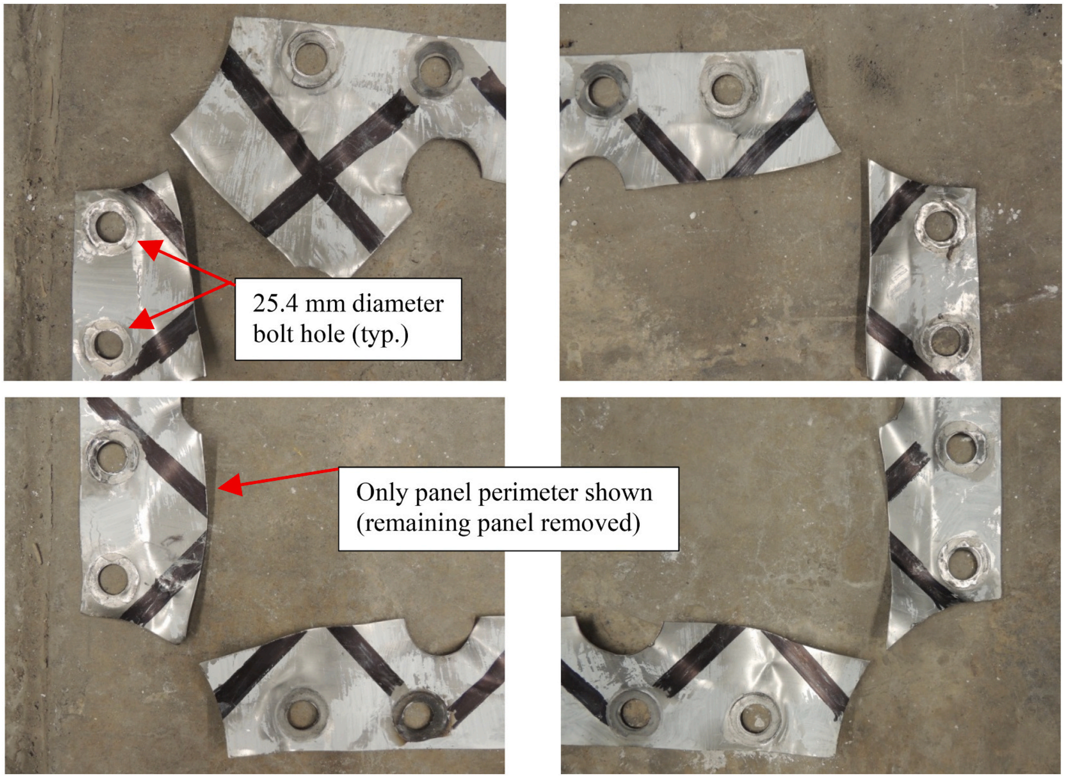


**Fig. 14.** Post-test 25.4 mm diameter bolt holes at infill web panel corners.

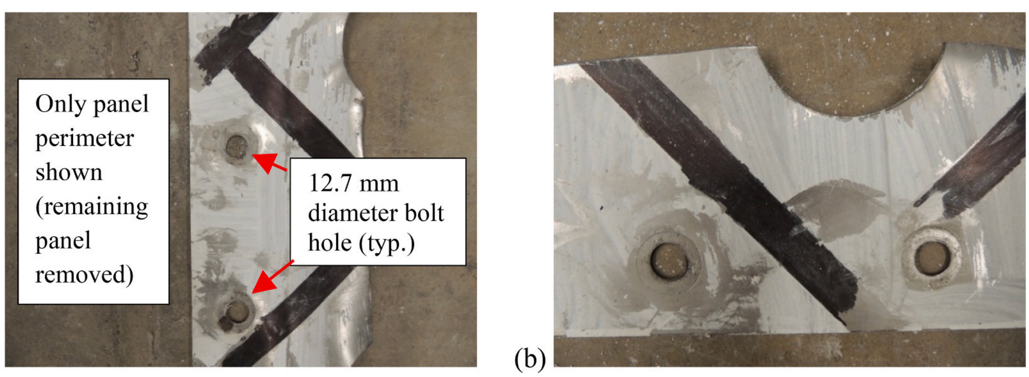


**Fig. 15.** Post-test 12.7 mm diameter typical bolt hole condition at infill web panel: (a) along VBE; (b) along HBE.

the performance of the slip-critical bolted component tension tests observed.

## Declaration of Competing Interest

The authors do not have any competing interests to declare.

## Acknowledgements

Funding for this collaborative project was provided by the National Science Foundation as part of the George E. Brown Network for Earthquake Engineering Simulation under award number CMMI-0830294. Steel for the boundary frame members was donated by the American Institute of Steel Construction. Additional financial support for D. Dowden was provided by MCEER. Any opinions, findings, conclusions, and recommendations presented in this paper are those of the authors and do not necessarily reflect the views of the sponsors. Furthermore, the authors would like to thank Robert Tremblay and Marie E. Gagné (former graduate student) of Ecole Polytechnique of Montreal for this collaboration and Eric Lachapelle of LAINCO Inc. for the perforated infill web panel donation.

## References

[1] J.W. Berman, M. Bruneau, Experimental investigation of light-gauge steel plate shear walls, J. Struct. Eng. 131 (2) (2005) 259–267.
[2] D. Vian, et al., Special perforated Steel plate shear walls with reduced beam section anchor beams. I: experimental investigation, J. Struct. Eng. 135 (3) (2009) 211–220.
[3] R. Purba, M. Bruneau, Finite-element investigation and design recommendations for perforated Steel plate shear walls, J. Struct. Eng. 135 (11) (2009) 1367–1376.
[4] AISC 341-10 Seismic Provisions for Structural Steel Buildings, ANSI/AISC American Institute of Steel Construction, Inc (AISC), Chicago, IL, 2010.
[5] M. Elgaaly, Thin steel plate shear walls behavior and analysis, Thin-Walled Struct. 32 (1) (1998) 151–180.
[6] D.J. Webster, J.W. Berman, L.N. Lowes, Experimental investigation of SPSW web plate stress field development and vertical boundary element demand, J. Struct. Eng. 140 (6) (2014), 04014011.
[7] M. Bruneau, C.-M. Uang, R. Sabelli, Ductile Design of Steel Structures, 2nd edition, McGraw-Hill Professional, 2011.

[8] AISI S100-12 North American Specification for the Design of Cold-Formed Steel Structureal Members, American Iron and Steel institute (AISI), 2012.
[9] AISC 360-10 Specification for Structural Steel Buildings, ANSI/AISC American Institute of Steel Construction, Inc (AISC), Chicago, IL, 2010.
[10] AISC 358s1-11 Prequalified Connections for Special and Intermediate Steel Moment Frames for Seismic Applications, including Supplement No. 1 (includes 2011 supplement), ANSI/AISC American Institute of Steel Construction, Inc (AISC), Chicagao, IL, 2011.
[11] P.M. Clayton, Self-Centering Steel Plate Shear Walls: Subassembly and Full-Scale Testing, in *PhD dissertation, Dept. of Civil and Environmental Engineering*, University of Washington, 2014.
[12] D.M. Dowden, M. Bruneau, Analytical and Experimental Investigation of Self-Centering Steel Plate Shear Walls, in *Tech. Rep. MCEER-14-0010*. Multidisciplinary Center for Earthquake Engineering Research, State University of New York Buffalo, Buffalo, New York, 2014.
[13] D.M. Dowden, M. Bruneau, Dynamic shake-table testing and analytical investigation of self-centering steel plate shear walls, J. Struct. Eng. 142 (10) (2016) 1–20.
[14] C. Christopoulos, et al., Posttensioned energy dissipating connections for moment-resisting steel frames, J. Struct. Eng. 128 (9) (2002) 1111–1120.
[15] M.M. Garlock, J.M. Ricles, R. Sause, Experimental studies of full-scale posttensioned steel connections, J. Struct. Eng. 131 (3) (2005) 438–448.
[16] J.M. Ricles, et al., Experimental evaluation of earthquake resistant posttensioned steel connections, J. Struct. Eng. 128 (7) (2002) 850–859.
[17] P. Rojas, J.M. Ricles, R. Sause, Seismic performance of post-tensioned steel moment resisting frames with friction devices, J. Struct. Eng. 131 (4) (2005) 529–540.
[18] D.M. Dowden, M. Bruneau, Quasi-static cyclic testing and analytical investigation of steel plate shear walls with different post-tensioned beam-to-column rocking connections, Eng. Struct. 187 (2019) 43–56.
[19] FEMA, State of the Art Report on Systems Performance of Steel Moment Frames Subject to Earthquake Ground Shaking: FEMA Rep. No. 355c, Federal Emergency Managment Agency, Washington, D.C, 2000.
[20] D.M. Dowden, M. Bruneau, NewZ-BREAKSS: post-tensioned rocking connection detail free of beam growth, AISC Eng. J. 48 (2) (2011) 153–158.
[21] D.M. Dowden, M. Bruneau, Kinematics of self-centering steel plate shear walls with NewZ-BREAKSS post-tensioned rocking connection, AISC Eng. J. 53 (3) (2016) 117–136.
[22] G. Clifton, et al., Sliding Hinge Joints and Subassemblies for Steel Moment Frames, in *NZSEE*, Palmerston North, New Zealand, 2007.
[23] H. Khoo, et al., Developments on the Sliding Hinge Joint, in *15WCEE*, 2012. Lisbon, Portugal.
[24] G.A. MacRae, G.C. Clifton, J.W. Butterworth, Some Recent New Zealand Research on Seismic Steel Structures, in *STESSA09*, 2009. Philadelphia, PA.
[25] T.J. Mander, et al., Damage avoidance design steel beam-column moment connection using high-force-to-volume dissipators, J. Struct. Eng. 135 (11) (2009) 1390–1397.
[26] ASTM Standard Specification for Structural Steel Shapes, ASTM A992/A992M-11, West Conshohocken, PA, 2015.
[27] ASTM Standard Specification for Low-Relaxation, Seven-Wire Steel Strand for Prestressed Concrete, ASTM A416/A416M-15, West Conshohocken, PA, 2015.
[28] ASTM Standard Specification for Steel, Sheet, Cold-Rolled, Carbon, Structural, High-Strength Low-Alloy, High-Strength Low-Alloy with Improved Formability, Required Hardness, Solution Hardened, and Bake Hardenable, ASTM A1008/A1008M, West Conshohocken, PA, 2015.
[29] D. Kusumastuti, A. Reinhorn, A. Rutenberg, A Versatile Experimentation Model for Study of Structures Near Collapse Applied to Seismic Evaluation of Irregular Structures, in Tech. Rep. MCEER-05-0002, Multidisciplinary Center for Earthquake Engineering Research, State University of New York Buffalo, Buffalo, New York, 2005.
[30] ASTM Standard Specification for Structural Bolts, Steel, Heat Treated, 120/105 ksi Minium Tensile Strength, ASTM A325-14, West Conshohocken, PA, 2014.
[31] P.M. Clayton, et al., Comparison of web plate numerical models for self-centering steel plate shear walls, Earthq. Eng. Struct. Dyn. 44 (12) (2015) 2093–2110.